L_{III}-edge spectroscopy on cerium-based intermediate-valent compounds

D. Malterre*
Institut de Physique, 1 rue Louis Bréguet, CH-2000 Neuchâtel, Switzerland
(Received 11 May 1990)

In this paper, the L_{III}-edge spectroscopy in cerium-based compounds is discussed in the framework of a single-impurity model. A few years ago, Gunnarsson and Schönhammer developed a model to describe photoemission in such systems. This model neglects the interaction between the photoelectron and the remaining system and then is not appropriate for L_{III} absorption. More recently, Jo and Kotani proposed an approach to describe the L_{III} edge of cerium oxide that accounts for the Coulomb interaction between the photoelectron, the f electron, and the core hole. I present a modification of this model by introducing a hybridization term between the photoelectron and the conduction states. A better agreement with experiment is then obtained for intermetallic compounds. Moreover, the phenomenological approach of the L_{III} edges used by most experimentalists is discussed.

I. INTRODUCTION

In many compounds, cerium exhibits unusual physical properties (magnetism, specific heat, resistivity, etc.) that are connected to the anomalies of its electronic configuration.[1] It has been shown that these pathological behaviors are due to a partial delocalization of the $4f$ electrons, which leads to a Kondo or an intermediate-valent (IV) ground state.

In the last decade, a large number of high-energy spectroscopic measurements [x-ray (XPS) or uv photoemission, x-ray absorption, electron-energy loss, etc.] have evidenced that the spectra of IV compounds exhibit satellites that cannot be explained in a simple one-electron picture.[2] Then many-body models have been developed to understand the experimental results. Up to now, the Gunnarsson-Schönhammer (GS) model[3,4] based on an Anderson-impurity Hamiltonian appears to be the most powerful approach. In the initial state the ground state is described by an N_f degenerate Anderson Hamiltonian using the $1/N_f$ expansion technique.[5] As the satellite structures are thought to be due to the relaxation of $4f$ electrons in the core-hole potential, this model explicitly introduces an attractive Coulomb potential between the core hole and the $4f$ electrons in the final state. The spectral function is then obtained in the sudden approximation by using the golden rule. The main parameters of the Hamiltonian (i.e., the position of the $4f$ electrons, the $4f$ intra-atomic Coulomb interaction, and the strength of hybridization between $4f$ and conduction states) can be estimated by fitting theoretical spectra to experimental results. This model can reproduce different spectroscopic measurements with the same set of parameters: core-level (essentially on the Ce $3d$ level) and valence-band photoemission, and bremstrahlung isochromat spectroscopy (BIS).[6] In the early 1980s, the spectroscopic techniques have provided fundamental new results with respect to the traditional techniques by giving specific information on the microscopic aspect of valence fluctuations: (i) a systematic study of Ce $3d$ XPS spectra in compounds with transition metals (Co, Ni, Ru, etc.) that were previously considered tetravalent ($n_f=0$) by the macroscopic experimental techniques (susceptibility, specific heat, etc.) has shown that their $4f$ occupation number is larger than 0.8;[7] (ii) the hybridization strength is 1 order or magnitude larger (100 meV) than the value deduced from thermodynamic measurements; and (iii) the $4f$ energy level is deeper than previously thought (about -2 eV with respect to the Fermi level).

On the other hand, x-ray-absorption spectroscopy (XAS) at the L_{III} edge has also been widely used to study IV materials.[8–13] This spectroscopy is a bulk technique and does not require ultrahigh vacuum as do photoemission and BIS. However, from a theoretical point of view, it is more complicated because the interaction in the final state between the photoelectron and the system cannot be neglected. Thus the GS model is not appropriate to describe such experiments. To illustrate the differences between XAS and XPS spectroscopies, I have reported in Fig. 1 the Ce $3d$ photoemission spectrum and the L_{III} edge of a strongly-mixed-valent alloy.[14] Two series of lines appear in the photoemission spectrum due to the spin-orbit ($3d^{5/2}$ and $3d^{3/2}$) separation. Three components are clearly shown for each series and are interpreted in terms of final states of mainly $4f^2$, $4f^1$, and $4f^0$ character. They result from the interaction of the $4f$ electrons with the core hole. In particular, the "$4f^2$" satellite can be understood as follows:[15] Owing to a large hybridization, the ground state is a mixture of mainly $4f^1$ and $4f^0$ configurations—the $4f^2$—well above the others in energy—does not significantly contribute, but the presence of a core hole in the final state leads to a lowering of the energy of this configuration, which becomes lower than the $4f^1$ and $4f^0$ ones. By contrast, the L_{III}-edge spectrum exhibits two white lines. Up to now, only phenomenological approaches are used by experimentalists to deduce the $4f$ occupation number from these XAS experiments. The two lines are interpreted as $2p^54f^1$ and $2p^54f^0$ final states, and the average valence is simply obtained from the relative intensity of the two edges.[16] This

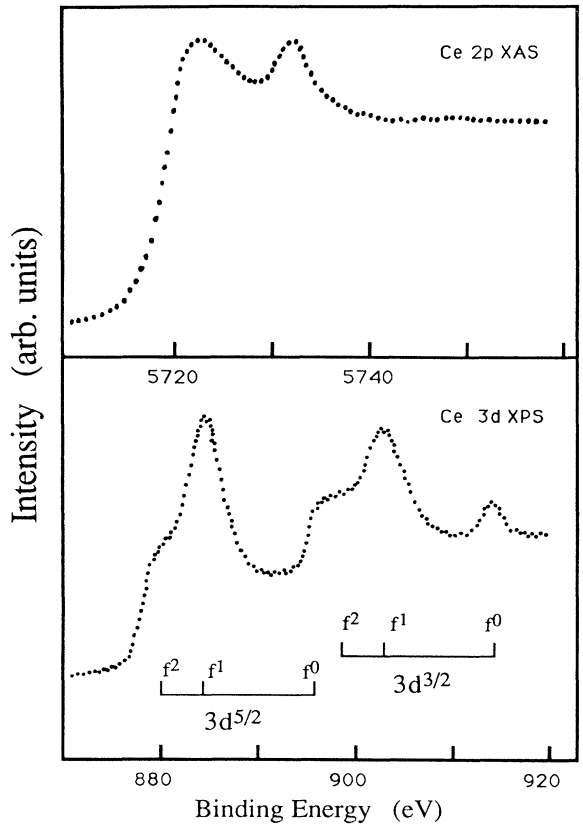

FIG. 1. X-ray absorption at the L_{III} edge and x-ray photoemission on the Ce $3d$ level for the $Pd_{0.86}Ce_{0.14}$ alloy (Ref. 14); the main structures of these two spectra are aligned.

interpretation was often criticized and, according to some authors, the average valence determined in this way has no physical meaning.[17] Delley and Beck[18] applied the GS model and suggested that the L_{III}-edge spectra can be considered a simple convolution of the photoemission spectrum, with a one-electron function describing the density of final states and the transition-matrix elements. In this approach, two broad structures appear in the calculated spectra: The main peak is constituted by the "$4f^2$" and "$4f^1$" final states (not resolved because of the important linewidth in $2p$ XAS). The L_{III} edge is qualitatively reproduced by this convolution procedure, but a shoulder, not observed experimentally, appears at the threshold in the calculated spectra. Moreover, the energy separation between the two main structures is overestimated.

More recently, Kotani and Coll[19–21] have pointed out that the differences between XAS and XPS spectroscopies result from the interaction between the photoelectron and the remaining system, which is not taken into account in the GS model. In photoemission spectroscopy this interaction can be neglected owing to the high energy of the photoelectron, but it is more questionable in XAS (the kinetic energy of the photoelectron being very low near the edge). The core-hole potential will localize the photoelectron and strongly modify the final states with respect to photoemission. These authors have shown that the introduction of this interaction in the Hamiltonian leads to an L_{III} edge with only two structures, and reproduces fairly well the experimental spectra of insulators (CeO_2).

The aim of this paper is to discuss the cerium L_{III}-edge spectroscopy in metallic systems and its possible description in the framework if a single-impurity model. In Sec. II, the model of Jo and Kotani,[19] which is known to give a satisfactory agreement with experiments in the case of insulators, is briefly recalled. An extension to their Hamiltonian is proposed for a better description of metallic systems. In Sec. III the influence of the different parameters is analyzed. It is shown that the Jo-Kotani model does not quantitatively reproduce the spectra of intermetallic compounds, and that the introduction of the hybridization between the localized photoelectron and the conduction states leads to a better agreement with experiment. Finally, in Sec. IV the phenomenological approach of the L_{III} edge used by most experimentalists is discussed in the light of this impurity model. It is demonstrated that, although the ratio of the intensities of the two structures in the L_{III} edge is not rigorously equal to the $4f$ occupation number, this phenomenological approach provides information concerning the configuration mixing of the ground state and then keeps a physical meaning.

II. MODEL

Let us briefly discuss the model developed by Gunnarsson and Schönhammer[3] to describe the high-energy spectroscopy measurements on cerium compounds. This model is based on a modified single-impurity Anderson Hamiltonian,[22] where a degenerate f orbital is embedded in a conduction band. The localized f states (energy ε_f) are characterized by strong intra-atomic correlations and are coupled to the conduction states by a hybridization term. In the final state, the Hamiltonian is modified by the Coulomb interaction ($-U_{fc}$) between the f electrons and the core-hole potential: ε_f must be replaced by $\varepsilon_f - U_{fc}$.

In the initial state, the Hamiltonian is

$$H_0 = \sum_k \varepsilon_k a_k^\dagger a_k + \varepsilon_f \sum_m a_m^\dagger a_m + U_{ff} \sum_{m,m'} n_m n_{m'} + \sum_{k,m} \frac{V_{km}}{\sqrt{N}} a_m^\dagger a_k + \text{c.c.} ,$$

where a_k and a_m are the destruction operators of conduction and f electrons respectively, V_{km} is the matrix element of the hybridization between k and f states (degeneracy N_f), and U_{ff} describes the Coulomb interaction between f states.

The ground state $|\Psi_0\rangle$ of this Hamiltonian can be calculated by variational or perturbation methods.[3] Following an idea of Anderson developed by Ramakrishnan *et al.*,[5] GS have used a $1/N_f$ expansion to calculate the ground state of this Hamiltonian. The first-order solution is exact in the limit of infinite degeneracy, and provides a good approximation for cerium; $N_f = 14$ if the spin-orbit is neglected. The ground state can be written as

$$|\Psi_0\rangle = A_0 \left[1 + \sum_{m,k} C_{m,k} a_m^\dagger a_k + \sum_{m,m',k,k'} B_{m,m';k,k'} a_m^\dagger a_{m'}^\dagger a_k a_{k'} \right] |\Phi_0\rangle \ .$$

$|\Phi_0\rangle$ corresponds to the state with f states empty and conduction states occupied up to the Fermi level: $|\Phi_0\rangle = \prod_k a_k^\dagger |0\rangle$; the second and third terms describe states with one f electron and a hole in the conduction band, and states with two f electrons and two holes in the conduction band, respectively (only occupied states are considered in the summation and in the product). The ground state is then a mixture of three configurations: $4f^1$, $4f^0$ and $4f^2$.

A. Many-body response to the core-hole potential

In this paper, the alternative method developed by Kotani *et al.* (a direct diagonalization of the Hamiltonian in a restricted basis set) will be used to obtain the different states. Let us recall the principle of this calculation (see the review of Kotani *et al.*[21]). The conduction band is discretized: $\varepsilon_k = -n\,W/N$ with $0 \le n \le N$. The normalized basis states are defined as

$$|f^0\rangle = |\Phi_0\rangle \ ,$$

$$|f^1, \bar{k}\rangle = \left[\frac{1}{N_f} \right]^{1/2} \sum_m a_m^\dagger a_k |\Phi_0\rangle \ ,$$

$$|f^2, \bar{k}_1, \bar{k}_2\rangle = \left[\frac{1+\delta_{k_1,k_2}}{N_f(N_f-1)} \right]^{1/2} \sum_{m,m'} a_m^\dagger a_{m'}^\dagger a_{k_1} a_{k_2} |\Phi_0\rangle \ .$$

These states represent the $4f^0$, $4f^1$, and $4f^2$ configurations ($\bar{k}$ is a hole in the conduction band).

The matrix elements of H_0 are given, for *diagonal elements*, by

$$\langle f^0|H_0|f^0\rangle = E_0 = 0 \ ,$$

$$\langle f^1, \bar{k}|H_0|f^1, \bar{k}\rangle = \varepsilon_f^0 - \varepsilon_k \ ,$$

$$\langle f^2, \bar{k}_1, \bar{k}_2|H_0|f^2, \bar{k}_1, \bar{k}_2\rangle = 2\varepsilon_f^0 - \varepsilon_{k_1} - \varepsilon_{k_2} + U_{ff} \ ;$$

and, for *nondiagonal elements* ($V_f = V_{km}$), by

$$\langle f^1, \bar{k}|H_0|f^0\rangle = V_f \left[\frac{N_f}{N} \right]^{1/2} \ ,$$

$$\langle f^2, \bar{k}_1, \bar{k}_2|H_0|f^1, \bar{k}'\rangle = V_f \left[(\delta_{k_1,k'} + \delta_{k_2,k'}) \frac{N_f - 1}{N} \right]^{1/2} .$$

In the final state, a core hole is located on the cerium ion and interacts with the $4f$ electrons. As noticed above, to give a correct description of the L_{III} edge, Kotani *et al.* have introduced the interactions between the photoelectron and the remaining system. They assumed that the $5d$ photoelectron is subjected to an attractive core-hole potential ($-U_{dc}$) and is coupled to the different $4f$ configurations by a repulsive interaction (U_{fd}). Then the Hamiltonian in the final state is written as

$$H' = H_0 + \varepsilon_c n_c - U_{fc} n_c \sum_m n_m + U_{fd} n_d \sum_m n_m + (\varepsilon_d - U_{dc}) n_d n_c \ .$$

Actually, I used a simplified version of the Kotani Hamiltonian. Whereas a set of photoelectron states of different energies is introduced by Kotani *et al.*, I assume that the photoelectron goes in a nondegenerate localized d state of energy ε_d.

As will be shown in the next section, this Hamiltonian cannot quantitatively explain the experimental spectra of intermetallic compounds; thus I add a new term to the Hamiltonian:

$$H'' = \sum_{k<k_F} V_{kd} a_d^\dagger a_k + \text{c.c.}$$

This term describes the hybridization between the photoelectron and the conduction states below the Fermi level. In the final state, owing to the Coulomb interaction with the core hole ($-U_{dc}$), the photoelectron is localized on the absorbing atom. This localization of the photoelectron was previously suggested from an experimental point of view by systematic studies of the L_{III} edge in cerium compounds which show that the energy position is nearly insensitive to effects of the solid-state environment.[23,24] In the following, this point will be discussed in more detail. The localized $5d$ photoelectron hybridizes with the conduction electron as the $4f$ electrons do. As the photoelectron will be more extended than the $4f$ electrons, V_{kd} must be greater than V_{kf}. For simplicity, the hybridization is restricted to states below the Fermi level. Then, this new term H'' couples states with holes in the conduction band; the basis states used by Kotani *et al.* must be extended. To diagonalize the final-state Hamiltonian, let us introduce a new basis corresponding to excited states with a core hole and a photoelectron in a $5d$ orbital:

$$|f^0, d, \bar{c}\rangle = a_d^\dagger a_c |f^0\rangle \ ,$$

$$|f^1, \bar{k}, d, \bar{c}\rangle = a_d^\dagger a_c |f^1, \bar{k}\rangle \ ,$$

$$|f^2, \bar{k}_1, \bar{k}_2, d, \bar{c}\rangle = a_d^\dagger a_c |f^2, \bar{k}_1, \bar{k}_2\rangle \ .$$

When the hybridization between the photoelectron and the conduction states is included ($V_{kd} \neq 0$), this basis must be extended:

$$|f^1, 0, 0, \bar{c}\rangle = a_k^\dagger a_d |f^1, \bar{k}, d, \bar{c}\rangle \ ,$$

$$|f^2, \bar{k}_1, 0, \bar{c}\rangle = a_{k_2}^\dagger a_d |f^2, \bar{k}_1, \bar{k}_2, d, c\rangle \ .$$

(The 0 means that there is no d electron and/or hole in the conduction states.)

The matrix elements of $H_f = H' + H''$ are then given, for the *diagonal elements*, by

$$\langle f^0,d,\bar{c}|H|f^0,d,\bar{c}\rangle=(\varepsilon_d-U_{dc}),$$

$$\langle f^1,\bar{k},d,\bar{c}|H|f^1,\bar{k},d,\bar{c}\rangle = \varepsilon_f^0-\varepsilon_k+U_{fc}+(\varepsilon_d-U_{dc})+U_{fd} ,$$

$$\langle f^2,\bar{k}_1,\bar{k}_2,d,\bar{c}|H|f^2,\bar{k}_1,\bar{k}_2,d,\bar{c}\rangle = 2\varepsilon_f^0-\varepsilon_{k_1}-\varepsilon_{k_2}+U_{ff}-2U_{fc}+(\varepsilon_d-U_{dc})+2U_{fd} ,$$

$$\langle f^1,0,0,\bar{c}|H|f^1,0,0,\bar{c}\rangle=\varepsilon_f^0-U_{fc} ,$$

$$\langle f^2,\bar{k},0,\bar{c}|H|f^2,\bar{k},0,\bar{c}\rangle=2\varepsilon_f^0-\varepsilon_k+U_{ff}-2U_{fc} ;$$

and, for *nondiagonal elements* ($V_d=V_{kd}$), by

$$\langle f^1,\bar{k},d,\bar{c}|H|f^0,d,\bar{c}\rangle=V_f\left[\frac{N_f}{N}\right]^{1/2} ,$$

$$\langle f^2,\bar{k}_1,\bar{k}_2,d,\bar{c}|H|f^1,\bar{k}',d,\bar{c}\rangle = V_f\left[(\delta_{k',k_2}+\delta_{k',k_1})\frac{N_f-1}{n}\right]^{1/2} ,$$

$$\langle f^1,\bar{k},d,\bar{c}|H|f^1,0,0,\bar{c}\rangle=V_d ,$$

$$\langle f^2,\bar{k}_1,\bar{k}_2,d,\bar{c}|H|f^2,\bar{k}',0,\bar{c}\rangle=(\delta_{k',k_2}+\delta_{k',k_1})V_d .$$

The eigenvectors of this Hamiltonian give the photoabsorption final states. The spectral function is then obtained by using the golden rule:

$$F_{\mathrm{XAS}}(\omega)\propto\sum_f|\langle\Psi_i|H_{\mathrm{int}}|\Psi_f\rangle|^2\,\delta(\hbar\omega-E_i+E_f) ,$$

where E_i and E_f are the energies of the ground state $|\Psi_i\rangle$ and of the different final states $|\Psi_f\rangle$, respectively, and H_{int} is the interaction Hamiltonian between the photon and the system. To take into account the finite lifetime of the core hole, a Lorentzian broadening of the spectra is introduced.

B. How to build an L_{III}-edge spectrum

In the preceding subsection, the N-body response to the creation of a core hole is derived. Mahan has shown that in the presence of many-body effects the absorption probability can be written as a convolution product of two functions that describe the one-electron contribution $B(\omega)$ and the many-body effects $F_{\mathrm{XAS}}(\omega)$ respectively:[25]

$$\mu(\omega)=\int F_{\mathrm{XAS}}(\varepsilon)B(\omega-\varepsilon)d\varepsilon . \quad (1)$$

Such a convolution relation has been explicitly demonstrated for the L_{III} edge of IV compounds by Hammoud *et al.*[26] in the limit $U_{fd}=U_{dc}=0$ (absence of interaction with the photoelectron). To model the one-electron absorption $B(\omega)$, the L_{III} edge of normal rare-earth elements can be considered. In such systems, the many-body effects on the L_{III} edge are negligible since the spectra (white lines) are correctly described with a one-electron–band calculation.[27] Besides, the shape of these "white lines" does not significantly depend on the details of the density of states and appears as a structureless peak a few eV wide. Then the L_{III}-edge spectrum of IV compounds will simply be obtained by convoluting the

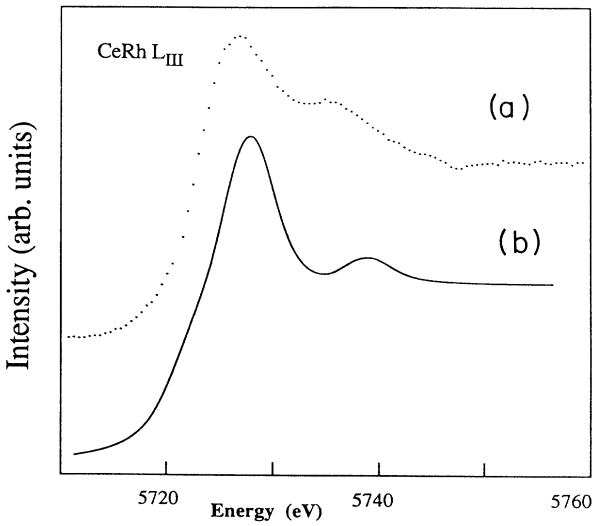

FIG. 2. (a) L_{III}-edge spectrum of the IV compound CeRh (Ref. 28). (b) Calculated spectrum in the limit $U_{fd}=U_{dc}=0$ with the convolution relation (1) ($V_f=0.35$ eV, $U_{ff}=7$ eV, $U_{fc}=10$ eV, and $\varepsilon_f=-1.5$ eV). A schematic (square) white line 4 eV wide has been chosen to model the one-electron function $B(\omega)$. The calculated spectrum is convoluted with a Gaussian and a Lorentzian of 3.5 and 2 eV width at half-height, respectively, to include finite lifetime and resolution.

$F_{\mathrm{XAS}}(\omega)$ function (in this limit it reduces to the photoemission spectral function) with a function simulating a schematic white line. The calculation leads to important disagreements with experimental results (Fig. 2): (i) the energy separation between the two main structures is overestimated (11 eV instead of 7 eV), and (ii) a shoulder appears in the threshold in the calculation. The calculation confirms the GS Hamiltonian is not appropriate and that the interactions between the photoelectron and the other electrons cannot be neglected in L_{III}-edge spectroscopy.

When these interactions are taken into account, the convolution relation (1) is no longer valid. The photoelectron and the other electrons cannot be separated and must be considered as a whole. Then, to describe the shape of the L_{III}-edge spectra, I shall assume that the final states can be separated in two sets.

(a) Final states with the photoelectron in a quasiatomic, *localized* 5*d* level; the different interactions (U_{fd}, U_{dc}, and V_d) must then be taken into account. The transitions towards these states give the resonant shape of the edge.

(b) Final states with the photoelectron in the *continuum* levels with an orbital angular momentum l equal to 0 or 2 according to the dipole selection rule. In this case the photoelectron is very delocalized and its interactions with the other electrons can be neglected, just as in photoemission experiments. As we will see, these transitions only contribute to the "background."

These two kinds of final states are clearly evidenced in the $M_{\mathrm{IV,V}}$ absorption spectroscopy (on the 3*d* level): the transitions towards the final localized 4*f* states gives reso-

nant lines, and are about 5 eV lower in energy with respect to the transitions towards the continuum. These latter transitions only give a structureless background.[29,30] In the L_{III}-edge spectroscopy, this distinction between two kinds of transitions is less clear. Nevertheless, several observations strongly suggest the localized character of the $5d$ photoelectron at the threshold. First, the L_{III} edge has a resonant shape that is usually considered an indication of localized final states. Moreover, in rare-earth elements, this shape does not depend on the nature of the material (metallic compounds, semiconductors, dilute solutions, or even the gaseous phase), corroborating the quasiatomic character of these transitions.[31] However, in contrast to $M_{IV,V}$, no energy separation is clearly detectable between the localized and continuum states, so it must not exceed 1 or 2 eV.

How do the transitions towards the continuum contribute to the absorption coefficient? This is a very delicate point. Kotani *et al.* only add a smooth background to their calculated spectra. I think that a more rigorous procedure can be used. Indeed, as the interactions between the photoelectron in a continuum state and the remaining system can be neglected, the contribution of these transitions is given by a convolution relation similar to Eq. (1). The corresponding spectral function is then calculated with the same parameters as those used to obtain the resonant line, except that all interactions involving the photoelectron (U_{fd}, U_{dc}, and V_d) vanish. Moreover, if the density of the continuum states is assumed to be constant above the Fermi level, and if the transition-matrix elements are energy independent, the $B(\omega)$ in (1) is a simple Heaviside step function. As seen in Fig. 3, these transitions give rise to a broad contribution. Finally, the total absorption coefficient is obtained by summing the two sets of final states (localized and continuum states) as illustrated in Fig. 4. The shift between the two contributions depends on the position—in energy—of the $5d$ photoelectron with respect to the Fermi level

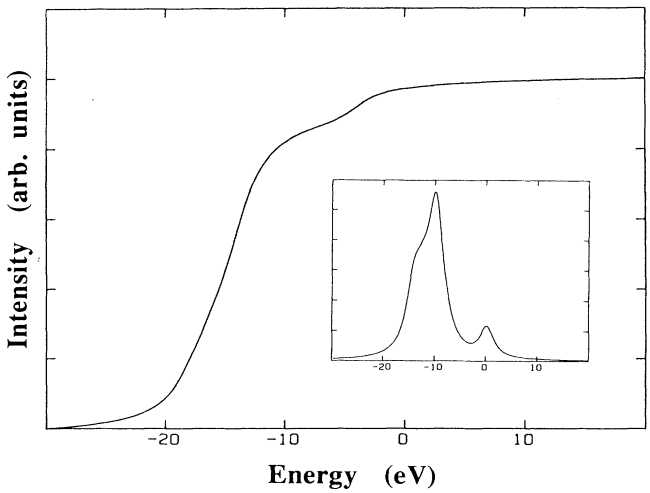

FIG. 3. Contribution of the transitions towards the continuum states. It is calculated from a convolution of the photoemission spectrum shown in the inset and a Heaviside step function.

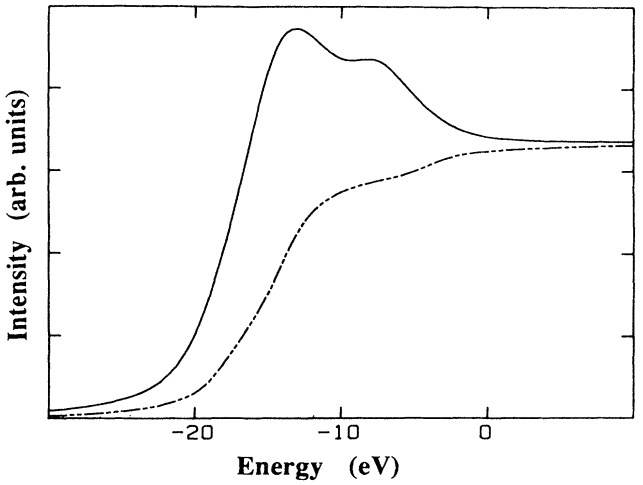

FIG. 4. The L_{III} edge is obtained by summing over all possible final states, localized $5d$ states, and continuum states (dashed line).

($\varepsilon_d - U_{dc}$). It can also be estimated experimentally from the comparison of the respective energy positions of XAS and XPS lines.

III. RESULTS

The influence of the different parameters of the model has been investigated. First, the effect of the Coulomb interactions between the photoelectron and the remaining system, introduced by Kotani *et al.*, has been analyzed. Because of these interactions, the calculated L_{III}-edge spectra only exhibit two structures, as is experimentally observed, but do not succeed to reproduce quantitatively their intensities in the case of strongly IV metallic compounds. Then, it is shown that when the hybridization term V_{dk} is introduced, better agreement with experiments is obtained.

The effect of U_{fd} on the $F_{XAS}(\omega)$ function is illustrated in Fig. 5. As only one d level is considered for the photoelectron, U_{dc} only shifts the energy scale. The other parameters are kept constant; they correspond to an IV ground state with a $4f$ occupation number of $n_f = 0.87$ ($\varepsilon_f = -1.5$ eV, $V_f = 0.3$ eV, $U_{ff} = 7$ eV, $U_{fc} = 10$ eV, and the width of the conduction band, $W = 3$ eV). As mentioned above, the spectrum with $U_{fd} = 0$ reflects the core photoemission spectrum with three structures, traditionally called the "$4f^2$", "$4f^1$", and "$4f^0$" satellites. With increasing U_{fd}, the positions and intensities of the satellites are modified and for $U_{fd} = 2-3$ eV, only two structures separated by about 9–10 eV are observed: the high-energy structure is mainly composed of the $4f^0$ final state, whereas the low-energy peak becomes a mixture of $4f^1$ and $4f^2$ final states. A similar behavior has already been shown for cerium oxide by Jo and Kotani;[19] nevertheless, in the latter case the hybridization is more important and both peaks are strongly mixed (cf. Fig. 2 of Ref. 18).

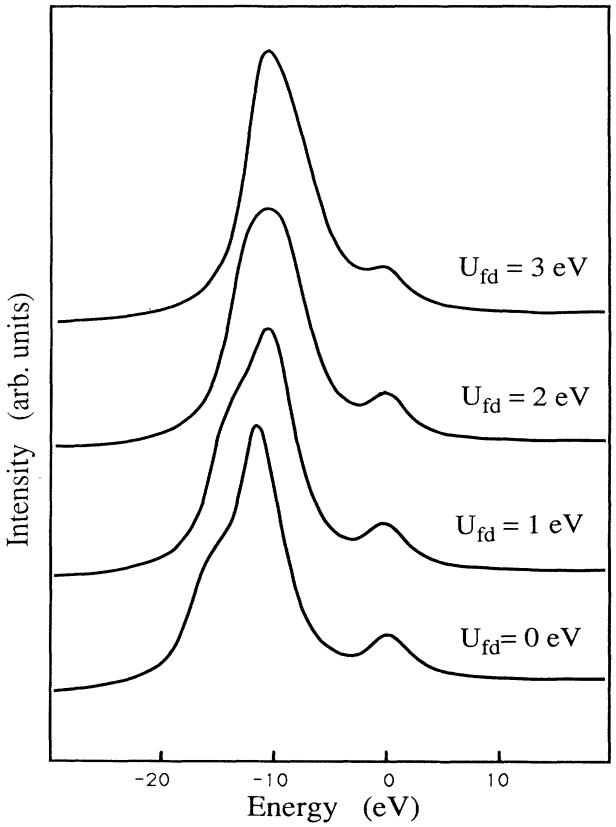

FIG. 5. $F_{XAS}(\omega)$ vs U_{fd} (the other parameters are left constant: $V_f=0.35$ eV, $U_{ff}=7$ eV, $U_{fc}=10$ eV, $\varepsilon_f=-1.5$ eV, $V_d=0$ eV, and $W=3$ eV). The $4f^1$ and $4f^2$ structures, well separated in the limit $U_{fd}=0$, mix with each other with increasing U_{fd}.

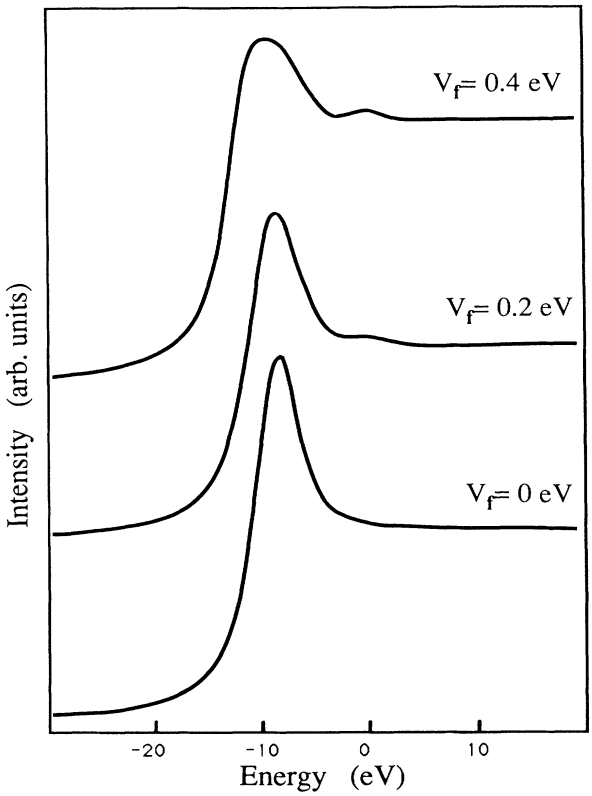

FIG. 6. L_{III}-edge spectra for several values of V_f with $U_{fd}=3$ eV, the other parameters remaining constant: $U_{ff}=7$ eV, $U_{fc}=10$ eV, $\varepsilon_f=-1.5$ eV, $V_d=0$ eV, and $W=3$ eV.

In Fig. 6, I have reported several spectra calculated in the framework of the Kotani model ($V_{kd}=0$ and $U_{fd}=3$ eV) for different values of the hybridization parameter between $4f$ and conduction electrons (V_f). For $V_f=0$, a single "white line" is observed, characteristic of the cerium trivalent configuration in the ground state (the final state is essentially $2p^5 4f^1 5d^1$). With increasing V_f, a second structure that corresponds to final state of $4f^0$ character appears at about 9–10 eV above the first threshold. Its intensity reflects the importance of the hybridization parameter, but remains weak even for strong hybridization. V_f is restricted to values less than 0.4 eV in order to be compatible with the photoemission spectrum. Thus, it seems that this model is not appropriate to describe the L_{III} edge of strongly-mixed-valent metallic materials like the Pd-Ce alloy (see Fig. 1). By contrast, it reproduces fairly well the edge of the CeO_2, as previously shown[18] (in this latter case, ε_f is 0.5 eV above the valence band, whereas its position with respect to the Fermi level is about -1.5 eV in metallic systems).

To obtain better agreement with experiments, the hybridization between the photoelectron and the conduction states must be added to the Hamiltonian. As the parameter V_{kd} is increased, an increase in the relative intensity of the second structure is observed; the L_{III}-edge spectra of strongly-mixed-valent materials exhibiting two structures of comparable intensity ($V_f>0.35$ eV) can be then reproduced. The best agreement is found for $V_{kd}=1.5$–2.0 eV. This value seems very large with respect to V_f (0.4 eV), but two complementary explanations can be proposed.

(i) The $4f$ level is degenerate, and then the hybridization is, in fact, $(N_f)^{1/2}V_f$, with $N_f=14$.

(ii) The $5d$ photoelectron is more delocalized than the $4f$ electrons, and thus its hybridization with the conduction states must be more important.

The parameter V_{kd} does not only affect the relative intensity of the two structures, but also their energy separation (for $V_d=2$ eV, this separation is about 7 eV). Moreover, the shapes of the two structures are different. The first structure of the calculated edge appears broader than the second, as was often observed in intermetallic compounds.[12–14]

IV. DISCUSSION OF THE PHENOMENOLOGICAL APPROACH

Let us now briefly discuss the usual phenomenological approach of the L_{III}-edge spectroscopy (a detailed discus-

sion can be found in Ref. 10). The two-bump structure in the IV materials is interpreted as a superposition of two white lines associated with the final $2p^5 4f^1$ and $2p^5 4f^0$ states, respectively (the $2p^5 4f^2$ configuration is ignored). The separation in energy is about 7–10 eV and is thought to originate from the screening of the core-hole potential by the localized $4f$ electron. Each white line is built from two contributions: a function that describes the transitions to the localized $5d$ states, and an arctan function that describes the transitions towards the continuum states. The $4f$ occupation number is simply obtained from the relative intensity of the two white lines. As discussed in this paper, a calculation based on an impurity Anderson Hamiltonian shows that such an approach is an oversimplified interpretation of the L_{III} edge: The two structures are not pure $2p^5 4f^1$ and $2p^5 4f^0$ final states, and, then, the $4f$ occupation number obtained from this fitting procedure is questionable. Nevertheless, to investigate the relation between the respective intensities of the two structures in the L_{III} edge and the electronic configuration in the ground state, I have fitted the calculated spectra with the phenomenological model for different V_f and then with different $4f$ occupation numbers (n_f). Then, it is possible to compare the n_f values given by the calculation with n_{XAS}, the relative intensity of the two structures given by the fitting procedure. In Fig. 7 several calculated spectra with $V_{kd}=2$ eV (dotted curves) are reported for different values of V_f. The lines result from the fitting procedure with the phenomenological approach. When the hybridization between $4f$ and conduction electrons increases, n_f progressively decreases and a second structure appears in the spectrum. The intensity of this structure qualitatively follows the evolution of n_f: it increases when n_f decreases. In Fig. 8 the occupation number is plotted as a function of n_{XAS}. One can see that there is no exact correspondence between the two sets of values, as was assumed in the phenomenological approach: n_f is always greater than n_{XAS}; the fitting procedure overestimates the valence admixture. Nevertheless, there is a linear relation between these two quantities. Although the fitting procedure is an oversimplified approach (the assumed final-state configurations are not correct), the respective intensities of the two structures reflect the configuration mixing in the ground state.

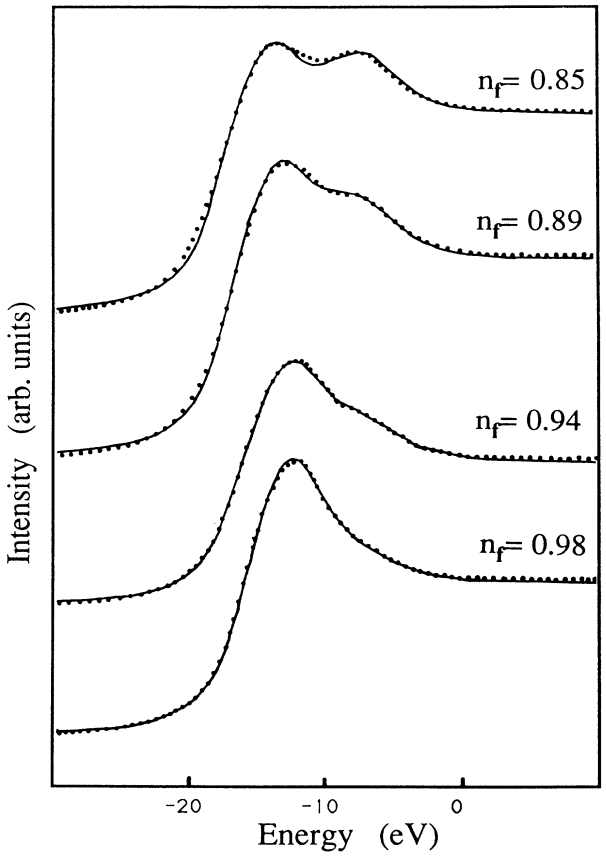

FIG. 7. Dotted curves show calculated L_{III}-edge spectra for several values of V_f from 0.1 to 0.4 eV (the other parameters are left constant: $U_{ff}=7$ eV, $U_{fc}=9$ eV, $\varepsilon_f=-1.5$ eV, $V_d=2.0$ eV, $U_{fd}=3$ eV, $W=2.5$ eV, and $\varepsilon_d-U_{dc}=-5$ eV; the calculated occupation of the $4f$ orbital, n_f, is indicated for each spectrum). The lines result from fits with the phenomenological approach. The calculated spectra are convoluted with a Gaussian and a Lorentzian 3.5 and 2 eV width at half-height, respectively, to include finite lifetime and resolution.

To compare this result with experiment, values of n_{XAS} and n_f found in the literature for several compounds are reported in the same figure: the values of n_{XAS} are obtained from the phenomenological fitting of the L_{III} edge,[32] whereas the n_f values are deduced from a Gunnarsson-Schönhammer fitting of XPS or BIS experiments.[6,33] Comparison between the two sets of values shows the same systematic trend: the empirical fitting of

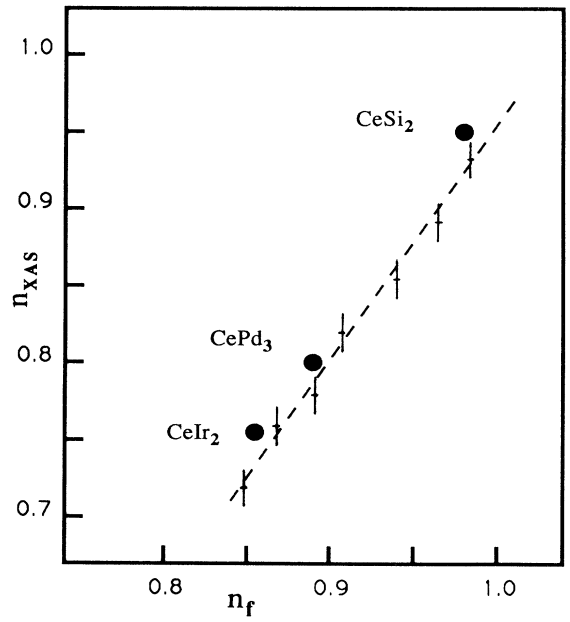

FIG. 8. $4f$ occupation number as a function of the respective intensity of the two L_{III}-edge structures of the calculated spectra. A linear relation is clearly shown (dashed line). Experimental values for different compounds are also reported (solid circles).

the L_{III} edge overestimates the valence deduced from an elaborate many-body model of photoemission experiments. Then, the model developed in this paper gives a satisfactory description of L_{III} absorption measurements with ground-state parameters compatible with those deduced from other spectroscopic techniques.

V. CONCLUSIONS

In this paper the L_{III}-edge spectroscopy on IV compounds is discussed in the framework of a single-impurity model. As previously pointed out by Kotani *et al.*, the Coulomb interactions (U_{fd} and U_{fc}) between the photoelectron and the remaining part of the system cannot be neglected in contrast to photoemission spectroscopy. These interactions, which are ignored in the XPS model of GS (owing to the important kinetic energy of the photoelectron), lead to spectacular results: Whereas the XPS spectra exhibit three well-resolved structures, only two structures are observed in XAS. I have shown that the introduction of these interactions cannot quantitatively reproduce the edges of strongly-mixed-valent intermetallic compounds. I have extended the Kotani model by introducing a new term in the Hamiltonian that describes the hybridization between the photoelectron that is considered a localized state and the conduction electrons. Good agreement with experiment is then obtained. Finally, I have discussed the phenomenological approach used by experimentalists. It is shown that the assumptions concerning the final states in this approach are not correct, but the respective intensities of these structures are nevertheless proportional to the $4f$ occupation number, and thus reflect the electronic configuration in the ground state.

ACKNOWLEDGMENTS

The author wishes to thank Dr. C. Brouder and Professor G. Krill for fruitful discussions, an Dr. R. Stumm von Bordwehr for a critical reading of the manuscript.

---

*Permanent address: Laboratoire de Physique du Solide, Boîte Postale 239, 54506 Vandoeuvre lès Nancy, CEDEX, France.

[1]J. M. Lawrence, P. S. Rieseborough, and R. D. Parks. Rep. Prog. Phys. **44**, 1 (1980).

[2]For a review, see *High Energy Spectroscopy,* Vol. 10 of *The Handbook of the Physics and Chemistry of Rare-Earths,* edited by K. A. Gschneider, L. Eyring, and S. Hüfner (North-Holland, Amsterdam, 1987).

[3]O. Gunnarsson and K. Schönhammer, Phys. Rev. Lett. **50**, 604 (1983); Phys. Rev. B **28**, 4315 (1983).

[4]O. Gunnarsson and K. Schönhammer, Phys. Rev. B **31**, 4815 (1985).

[5]T. V. Ramakrishnan and K. Sur, Phys. Rev. B **26**, 1798 (1982).

[6]J. W. Allen and S. J. Oh, O. Gunnarsson, K. Schönhammer, M. B. Maple, M. S. Torikachvili, and I. Lindau, Adv. Phys. **35**, 275 (1986).

[7]J. C. Fuggle, F. U. Hillebrecht, Z. Zołnierek, R. Lässer, Ch. Freiburg, O. Gunnarsson, and K. Schönhammer, Phys. Rev. B **27**, 7330 (1983).

[8]H. Launois, M. Rawiso, E. Holland-Moritz, R. Pott, and D. Wohlleben, Phys. Rev. Lett. **44**, 1271 (1980).

[9]L. D. Finkel'shteyn and N. D. Samsonova, Fiz. Met. Metallovd. **53**, 718 (1982).

[10]R. D. Parks, S. Raaen, M. L. denBoer, V. Murgai, and T. Mihalisin, Phys. Rev. B **28**, 3556 (1983).

[11]D. Wohlleben and J. Röhler, J. Appl. Phys. **55**, 1904 (1984).

[12]E. Beaurepaire, G. Krill, J. P. Kappler, and J. Röhler, Solid State Commun. **49**, 65 (1984).

[13]R. A. Neifeld, M. Croft, T. Mihalisin, C. U. Segre, M. Madigan, M. S. Torikachvili, M. P. Maple, and L. E. Delong, Phys. Rev. B **32**, 6928 (1985).

[14]D. Malterre, G. Krill, J. Durand, and G. Marchal, Phys. Rev. B **38**, 3766 (1988).

[15]J. C. Fuggle, M. Campagna, Z. Zołnierek, R. Lässer, and A. Platau, Phys. Rev. Lett. **19**, 1597 (1980).

[16]J. Röhler, J. Magn. Magn. Mater. **47-48**, 175 (1985).

[17]W-D. Schneider, B. Delley, E. Wuilloud, J. M. Imer, and Y. Baer, Phys. Rev. B **32**, 6819 (1985).

[18]B. Delley and H. Beck, J. Magn. Magn. Mater. **47-48**, 269 (1985).

[19]T. Jo and A. Kotani, Solid State Commun. **54**, 451 91985).

[20]A. Kotani, J. Phys. (Paris) Colloq. **48**, C9-869 (1987).

[21]A. Kotani, T. Jo, and J. C. Parlebas, Adv. Phys. **37**, 37 (1988).

[22]P. W. Anderson, Phys. Rev. **124**, 41 (1961).

[23]J. M. Lawrence, M. L. denBoer, R. D. Parks, and J. L. Smith, Phys. Rev. B **29**, 568 (1984).

[24]B. Lengeler, G. Materlik, and J. E. Müller, Phys. Rev. B **28**, 2276 (1983).

[25]G. D. Mahan, in *Solid State Physics,* edited by H. Ehrenreich, F. Seitz, and D. Turnbull (Academic, New York, 1974), Vol. 29, p. 75.

[26]Y. Hammoud, J. C. Parlebas, and F. Gautier, J. Phys. F **17**, 503 (1987).

[27]G. Materlik, J. E. Müller, and J. W. Wilkins, Phys. Rev. Lett. **50**, 267 (1983).

[28]D. Malterre, C. Brouder, G. Krill, E. Beaurepaire, B. Carrière, J. P. Kappler, D. Chanderis, and H. Magnan, Nuovo Cimento (to be published).

[29]J. C. Fuggle, F. U. Hillebrecht, J.-M. Esteva, R. C. Karnatac, O. Gunnarsson, and K. Schönhammer, Phys. Rev. B **27**, 4637 (1983).

[30]G. Kaindl, G. Kalkowsky, W. D. Brewer, E. V. Sampathkumaran, M. Domke, and F. Holtzberg, J. Magn. Magn. Mater. **47-48**, 215 (1985).

[31]G. Materlik, B. Sonntag, and M. Tauch, Phys. Rev. Lett. **51**, 1300 (1983).

[32]J. Röhler, in *High Energy Spectroscopy* (Ref. 2), Chap. 71.

[33]F. Patthey, W. D. Schneider, Y. Baer, and B. Delley, Phys. Rev. Lett. **58**, 2810 (1987).